Recovery of bremsstrahlung photons in a FCC-ee detector

Emmanuel Perez[1*] and Michele Selvaggi[1*]

[1]CERN, Geneva, Switzerland.

*Corresponding author(s). E-mail(s): Emmanuel.Perez@cern.ch; Michele.Selvaggi@cern.ch;

1 Introduction

The physics studies performed in the context of the FCC-ee mid-term review report rely on Monte-Carlo events that were passed through a fast simulation of the IDEA detector using the DELPHES package. The tracking software of DELPHES relies on a full description of the tracker geometry. It accounts for the finite detector resolution and for the multiple scattering in the beam-pipe and in each tracker layer [1]. However, secondary interactions and bremsstrahlung radiation are not taken into account. Consequently, by default, the resolution of electron tracks is identical to that of muon tracks. As an implementation of bremsstrahlung radiation in DELPHES goes beyond the scope of this fast simulation framework, a more pragmatic approach has been chosen to account for bremsstrahlung, by applying an ad-hoc extra smearing to the momentum of electron tracks. The purpose of this study is to determine the parameters by which the DELPHES track resolution should be smeared, in order to represent the resolution that is expected for electrons. It uses an hybrid approach that combines a full GEANT4 simulation of single electrons in the tracker, with a simple model of bremsstrahlung recovery in a calorimeter. An efficient bremsstrahlung recovery puts some requirements on the electromagnetic calorimeter (resolution and granularity) which are briefly outlined and illustrated.

2 Simulation model

A full GEANT4 simulation of the IDEA detector, followed by some reconstruction software, is not in place yet. On the other hand, a full chain of GEANT4 simulation and of reconstruction exists for the CLD detector, making use of the `ILCSoft` software

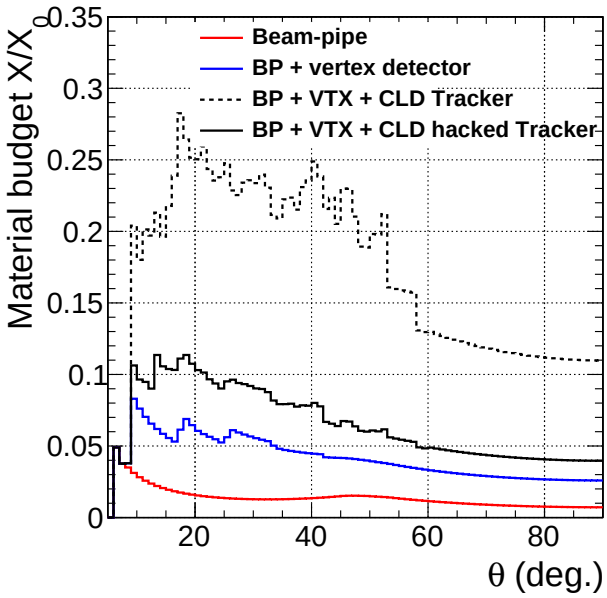

Fig. 1 Material budget in front of the electromagnetic calorimeter (full black curve), as used in the present study. The (lowest) red curve shows the material of the beam-pipe, and the (next-to-lowest) blue curve the material obtained when adding the vertex detector. For reference, the dashed curve shows the total material of the nominal CLD model.

chain. The CLD detector contains a full silicon tracker. Consequently, the amount of material that is crossed by particles going through the tracker volume is much larger than what it is in the very light drift chamber of the IDEA detector. In order to estimate the effect of bremsstrahlung in the IDEA detector, using the CLD full simulation framework, the description of the CLD main tracker has been "hacked" by artificially reducing the material of the layers of the main silicon tracker of CLD[1], such that the total material budget is similar to that of IDEA. The starting point for the detector model is the version `FCCee_o1_v04` of the CLD geometry, described in detail in [2]. For the barrel part, it contains a vertex detector, with three double-layers at radii between 17.5 and 58 mm, and the main tracker consists of six layers at radii of 13 cm, 49 cm, 67 cm, 1 m, 1.6 m and 2.1 m. The resulting material budget in X/X_0 of the "hacked" detector, as a function of the polar angle, is shown in Fig. 1 by the full black curve. It varies between $\sim 4\%$ in the central region and $\sim 10\%$ at forward angles. The tracker volume is immersed in a solenoidal field of 2 T. The reconstruction software is implemented in the `Marlin` framework. Only the reconstructed tracks are used here. Pattern recognition is done via the `ConformalTracking` algorithm, and the resulting tracks are fitted with a Kalman filter method. More details and references can be found in [2].

[1] That was achieved by reducing to a tiny value the thickness of the support structures, of the insulating layers, of the readout ASIC, etc. It is thus clear that such a "tracker" can not be built. The thickness of the sensitive silicon layers has been unchanged, such that the signal digitisation used for the default detector model can be kept unchanged.

3 Track momentum resolutions

Single electron events have been simulated and reconstructed with this setup, at fixed energy points, ranging between 1 GeV and 200 GeV and at fixed polar angles, between 10 and 89 degrees. Single muon events have also been produced for comparison.

3.1 Electron and muon track resolutions

The momentum resolution of muon tracks is shown in Fig. 2. For central muons of $20 - 100$ GeV, it agrees well with the muon momentum resolution obtained for IDEA with the DELPHES simulation shown in Ref. [1].

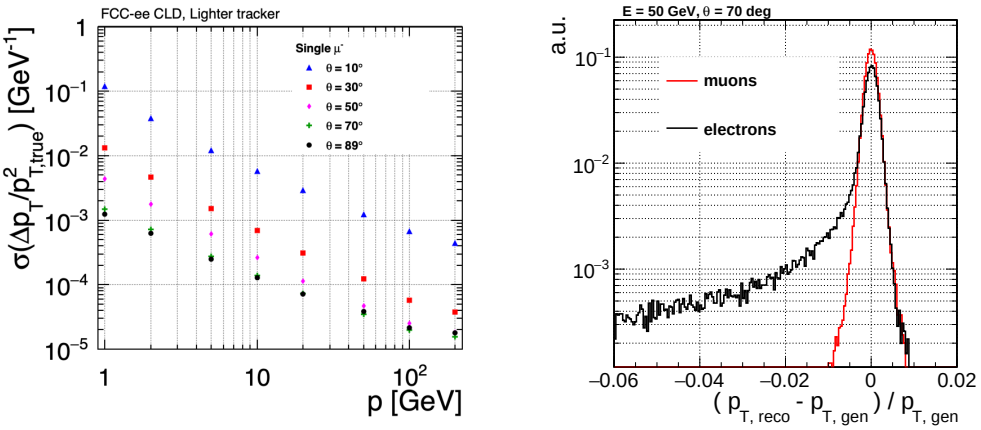

Fig. 2 Left: Momentum resolution of muons of various momenta and angles, obtained from a full simulation of the detector model described in the text. Right: Transverse momentum resolution of 50 GeV muons and electrons emitted at a polar angle of 70 degrees.

For electrons, the difference between the reconstructed track momentum, $p_{T,rec}$, and the generated momentum, $p_{T,gen}$, does not follow a Gaussian distribution because of the emission of bremsstrahlung photons, as illustrated in the right panel of Fig. 2. The normalised distribution of $(p_{T,rec} - p_{T,gen})$ is integrated in intervals around the peak of the distribution, and an effective resolution is defined as one half of the smallest interval for which the integral amounts to 68%. Compared to the muon momentum resolution, this effective electron resolution is larger by a factor of about two to four depending on the polar angle, as shown in Fig. 3.

3.2 Motivations for an improved electron resolution

An optimal electron momentum resolution is important for several measurements at the FCC-ee. To mention a few:

- the precise determination of the mass of the Higgs boson, M_H, from the distribution of the recoil mass in $Z(\ell\ell)H$ events [3]. Since the Higgs mass would need to be

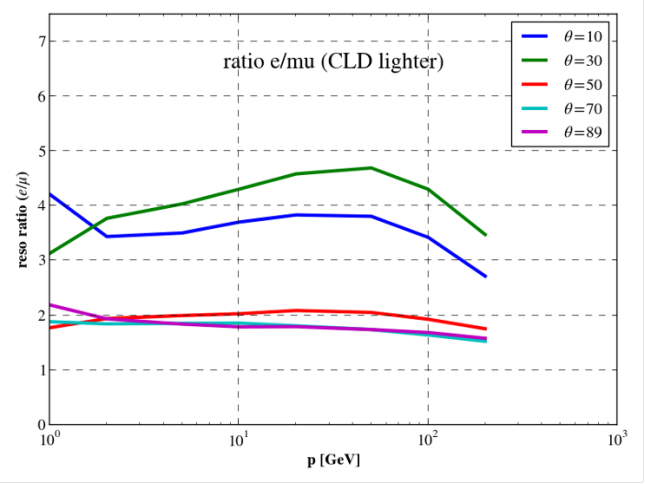

Fig. 3 Ratio of the effective resolution of electrons to the momentum resolution of muons as a function of the momentum, for several values of the polar angle. The effective resolution is defined as one half of the smallest interval for which the integral amounts to 68%.

measured to better than its intrinsic width in view of a potential resonant run at $\sqrt{s} = M_H$, an electron resolution as close as possible to the muon resolution would be a clear advantage. The degradation of the precision of the fitted Higgs mass when the electron momentum resolution is worsened is studied in [3].

- the search for lepton flavour violating decays of Z bosons into an electron and a tau lepton, using the huge statistics to be collected at the Z peak. The main background consists of $Z \to \tau\tau$ events where one τ decays into an electron that carries most of its momentum. The selection will require an identified τ recoiling against an electron whose momentum equals the beam energy, and the sensitivity varies linearly with the electron momentum resolution [4], the latter being ideally equal to the beam energy spread.

The electron momentum determination can be slightly improved by combining the track measurement with the independent measurement of the electron cluster provided by the electromagnetic calorimeter. In the energy range of interest at FCC-ee however, this improvement is limited. Further improvements can be brought by:

- a generalisation of the Kalman filter known as the Gaussian Sum Filtering technique (GSF) [5, 6], that accounts for the emission of bremsstrahlung photons in the layers crossed by the electron. This has been proven to be extremely powerful in the CMS tracker [7], for which the material budget is sizeable. However, in a detector where most of the material is located in the vertex detector (see Fig. 1), the majority of the bremsstrahlung photons are emitted at small radii (see Fig. 4), and the "pre-brem" component of the GSF track will be determined only from the first hits in the VXD, with a very poor resolution, because of the small number of hits and of the very limited lever arm. Consequently, the resolution of the GSF tracks is likely to be comparable to that of tracks fitted by the standard Kalman filter.

- a recovery, in the electromagnetic calorimeter, of the bremsstrahlung photons, whose energy is then added to the momentum of the track. This approach is pursued in the following section.

4 Recovery of bremsstrahlung photons

The generator-level information is used to retrieve the bremsstrahlung photons created by GEANT4. Figure 4 shows the radius at which these bremsstrahlung photons are created, for 50 GeV electrons emitted at 70 degrees - these values being "typical" of electrons in $Z(ee)H$ events. Peaks corresponding to the beam pipe radius and to the radial positions of the various detector layers are clearly visible.

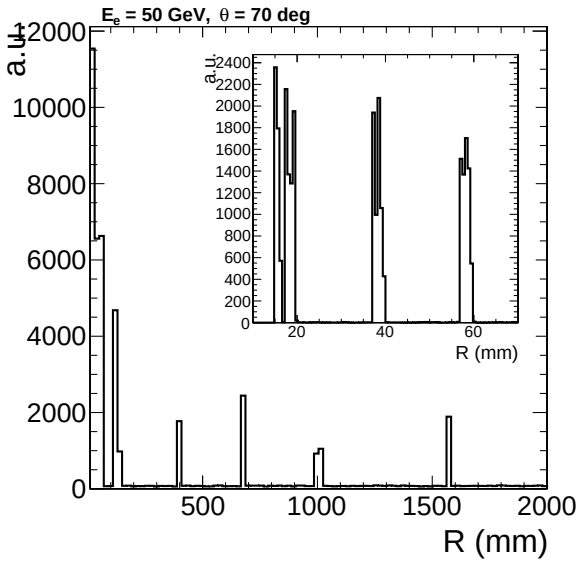

Fig. 4 Radial position of the production vertex of bremsstrahlung photons, for 50 GeV electrons emitted at a polar angle of 70 degrees. The insert is a zoom into the small radii region, that shows the peaks corresponding to the beam pipe and to the three double-layers of the vertex detector.

The multiplicity of bremsstrahlung photons is shown in the left panel of Fig. 5, for electrons of 50 and 20 GeV, emitted at an angle of 70 degrees. At this polar angle, about 65% of the electrons do not emit any bremsstrahlung photon. For these electrons, the momentum resolution has been checked to be identical, within a percent, to that of muons. On average, the total energy radiated by the bremsstrahlung photons, ΣE_γ, relative to the energy of the initial electron, is about 4.4%. At $\theta = 70°$, the amount of material that is crossed by the electron is 4.45% of a radiation length (see Fig. 1), hence this average energy is consistent with the expectation that $< \Sigma E_\gamma > \simeq t \times E_e$ where E_e is the electron energy and t the thickness of material traversed, in units of radiation length. Focusing on electrons that have emitted at least one photon, the distribution of the total energy that is radiated is depicted in the

right panel of Fig. 5, and the mean value of the radiated energy is about 12% of E_e.

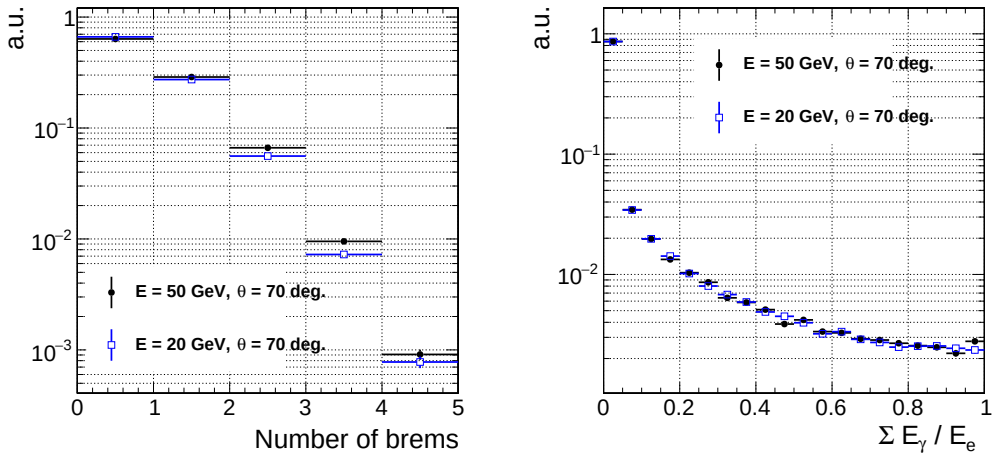

Fig. 5 Left: Multiplicity distribution of the bremsstrahlung photons, for electrons emitted at a polar angle of 70 degrees and for two values of their energy. Right: Distribution of the total energy radiated by the bremsshtrahlung photons, relative to the energy of the initial electron, for electrons that have radiated at least one photon.

4.1 Ideal recovery

For the 35% of 50 GeV electrons that radiate a photon, the radiated energy of $12\% \times E_e = 6$ GeV could ideally be measured with a resolution of $3\% \times \sqrt{E/\mathrm{GeV}} = 70$ MeV, in an electromagnetic calorimeter with a 3% stochastic term, as could be achieved with crystals. Since the bremsstrahlung emissions occur mostly in the first layers, the track of the post-brem electron is expected to be measured with a resolution similar to that of a muon of the same energy, σ_μ, which happens to also be about 70 MeV for $E = 50$ GeV and $\theta = 70°$. Consequently, by setting the reconstructed electron energy to $E_{rec} = \Sigma E_\gamma + p_{\mathrm{track}}$, the resolution on E_{rec} would be $\sqrt{2} \times \sigma_\mu$ for those electrons that have radiated a photon. Taking into account the electrons that do not emit any radiation, the average resolution for 50 GeV electrons at an angle of 70° would be worse than the muon resolution by only $\mathcal{O}(15\%)$. This estimate is consistent with the one presented in [8].

4.2 A more realistic recovery

The "ideal" estimates given above assume that the full radiated energy can be reconstructed. This is of course not the case. In particular, a radiated photon and the electron may be reconstructed in the same calorimeter cells or crystals, if their angular separation when they reach the ECAL surface is not large enough; and even if the two particles are separated at the ECAL entrance, their respective showers may overlap

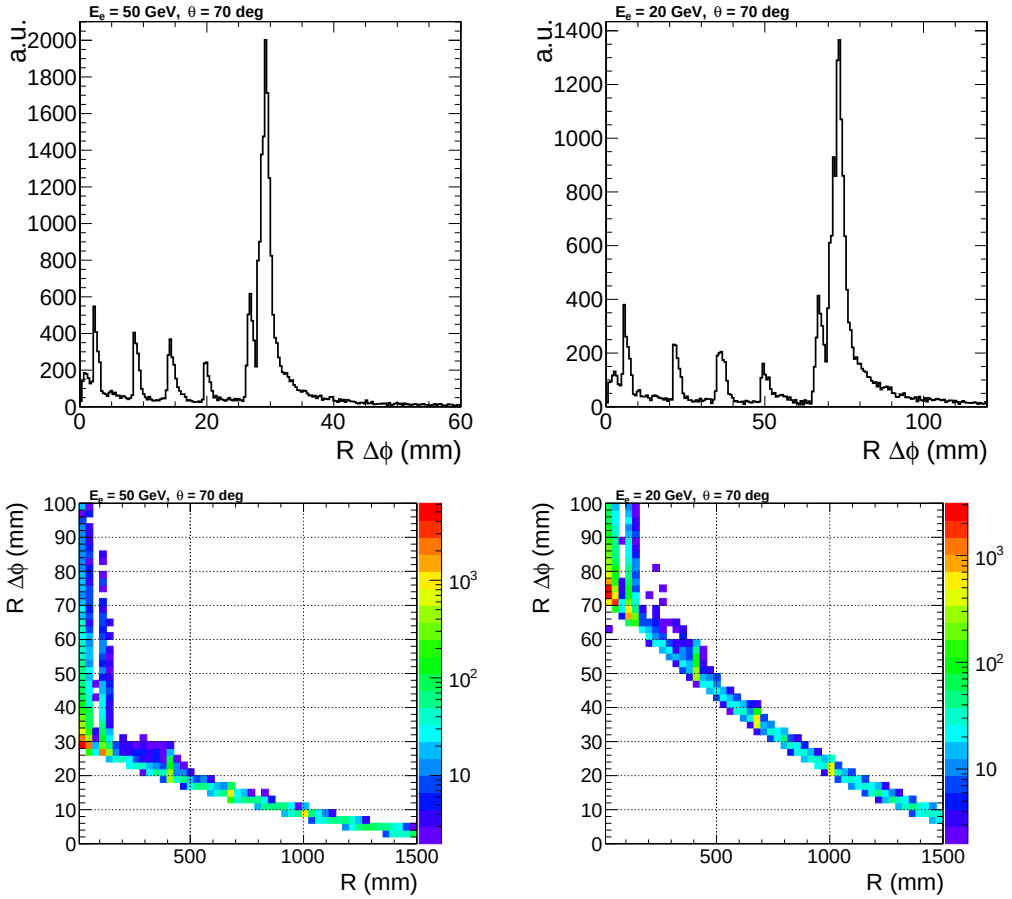

Fig. 6 Top: Distance in $R\phi$ between the electron track entry point at the ECAL and the radiated photons from GEANT4, for 50 GeV (left) and 20 GeV (right) electrons at $\theta = 70°$. Bottom: Correlation between the $R\phi$ distance between the electron and the photon, and the radius at which the photon has been radiated for 50 GeV (left) and 20 GeV (right) electrons at $\theta = 70°$.

when they develop in the calorimeter, which may prevent the reconstruction of the photon, or cause some energy to be swapped between the photon and the electron.

To take into account these effects, a simplified model for bremsstrahlung recovery has been used. In the $R\phi$ plane of the bending, the reconstructed "track state" of the electron at the interaction point (the tangent to its trajectory) is extrapolated, as a straight line, to the ECAL surface. This point, together with the entry point of the electron track at the ECAL surface, defines an angular window in azimuth, or in $R\phi$ where $R = 2.15$ m is the inner radius of the ECAL. All bremsstrahlung photons must hit the ECAL within this window. The simplified algorithm looks for the GEANT4

photons[2] that fall within this window and that are separated in $R\phi$ from the impact point of the electron by a minimum distance d_{min}, which is a parameter of the algorithm. The truth energy of these photons is smeared to account for the detector resolution, and, if the resulting energy is above a given threshold (typically the noise level in the calorimeter), it is added to the reconstructed radiated energy, ΣE_γ.

The top row of Fig. 6 shows the distance in $R\phi$ between the electron entry point at the ECAL and the radiated photons from GEANT4, for 50 GeV (left plot) and 20 GeV (right plot) electrons at $\theta = 70°$. For radiations that occur early, in the beam-pipe or in the vertex detector, the electron will bend in the 2 T magnetic field over a large distance, such that, when they reach the ECAL, the electron and the photon show a large separation in $R\phi$. That is the origin of the large peak, at $R\Delta\phi \sim 30$ mm in the top-left plot of Fig. 6. For electrons of 20 GeV (right plot), the bending of the electron trajectory is 2.5 times larger, and the separation between the electron and the photons, at the ECAL entrance, is about 75 mm. The smaller peaks seen at lower values of $R\Delta\phi$ correspond to emissions that occurred in the main tracker, at an increasing distance from the interaction point. The correlation between the $R\phi$ distance between the electron and the photon, and the radius at which the photon has been radiated, is shown in the lower row of Fig. 6.

Figure 7 shows the effective resolution obtained for 50 and 20 GeV electrons at $\theta = 70°$ with the bremsstrahlung recovery algorithm described above, normalised to the momentum resolution of muons at the same energy and angle. The ratio is shown as a function of the minimal distance d_{min} and for several assumptions on the energy resolution of the ECAL; the minimum threshold for reconstructing a radiated photon is set to 10 MeV.

For 50 GeV electrons (left plot), as long as d_{min} is smaller than about 25 mm, the large majority of the photons is reconstructed: only the photons that fall at $R\Delta\phi <$ 25 mm in the top left plot of Fig. 6 fail to be recovered. Consequently, the performance of the bremsstrahlung recovery reaches an asymptotic behaviour that is driven by the ECAL resolution. When d_{min} gets close to 30 mm, a quick degradation of the recovery is observed, and when d_{min} is larger than about 40 mm, the algorithm fails to reconstruct all the emissions (see again the top left plot of Fig. 6), and the observed resolution is basically equivalent to that obtained without any bremsstrahlung recovery (the ratio reaches ~ 1.9, consistent with Fig. 3). For 20 GeV electrons (right panel of Fig. 7), the same observations hold, the "transition" value of d_{min} being larger by a factor of 2.5, consistent with the larger bending of the electron.

Figure 8 shows how the bremsstrahlung recovery reduces the low energy tail in the distribution of $(p_{T,rec} - p_{T,gen})$. A calorimeter resolution of $3\%/\sqrt{E}$ has been used here, the energy threshold was set to 10 MeV, and a minimal $R\phi$ distance $d_{min} =$ 20 mm was assumed. In the left panel of Fig. 9, the energy threshold below which photons are not reconstructed was varied between 5 MeV and 100 MeV. It can be seen that the performance of the bremsstrahlung recovery depends little on the energy

[2]No attempt is made to recover the small fraction of radiated photons that convert into an electron-positron pair.

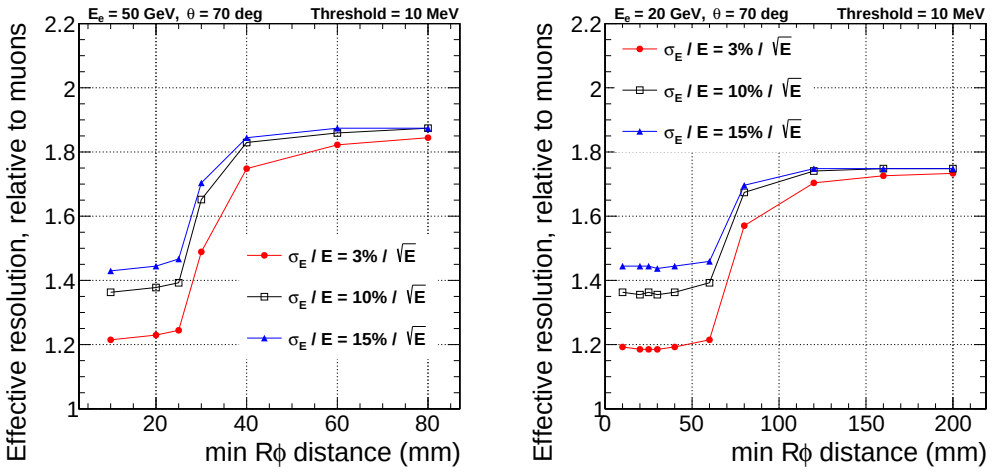

Fig. 7 Effective resolution of electrons relative to the muon momentum resolution, obtained with a bremsstrahlung recovery algorithm, for several assumptions on the energy resolution of the ECAL, and as a function of the minimum distance d_{min} in $R\phi$ between the electron and of the photon at the ECAL entrance, below which the radiated photons are not recovered.

threshold in this range. The right panel of Fig. 9 shows the angular dependence of the relative effective resolution for electrons of 50 GeV of energy, when the polar angle varies between 10° and 89°. The effective resolution for electrons, relative to the muon momentum resolution, does not depend much on the angle.

4.3 Conclusions and considerations on the detector

The bremsstrahlung recovery critically depends on the separation between the electron and the radiated photons when they reach the ECAL surface. A realistic value for the d_{min} parameter of the algorithm depends on the Moliere radius R_M of the ECAL, and of its granularity. The transverse granularity is usually set to be of the order of R_M or $0.5 \times R_M$; the longitudinal granularity helps in disentangling showers that partially overlap. An electron and a radiated photon that are separated by less than one Moliere radius in $R\phi$ when they reach the ECAL are unlikely to be separated by the reconstruction algorithm.

In a sandwich Si-W calorimeter as that foreseen for CLD, the Moliere radius can be as low[3] as 1.4 cm, a transverse granularity of 5×5 mm^2 can be achieved, and the ECAL consists of many longitudinal layers. Simulation studies and test beams of prototypes of the CALICE calorimeter show that a good separation of close-by electromagnetic showers can be achieved when they are more than $1 - 1.5 \times R_M$ apart [9]. Consequently, a value of about 20 mm for the d_{min} parameter of the recovery algorithm seems reasonable.

[3]The Moliere radius of tungsten is actually 0.9 cm, but the addition of silicon and gaps lead to a larger effective R_M.

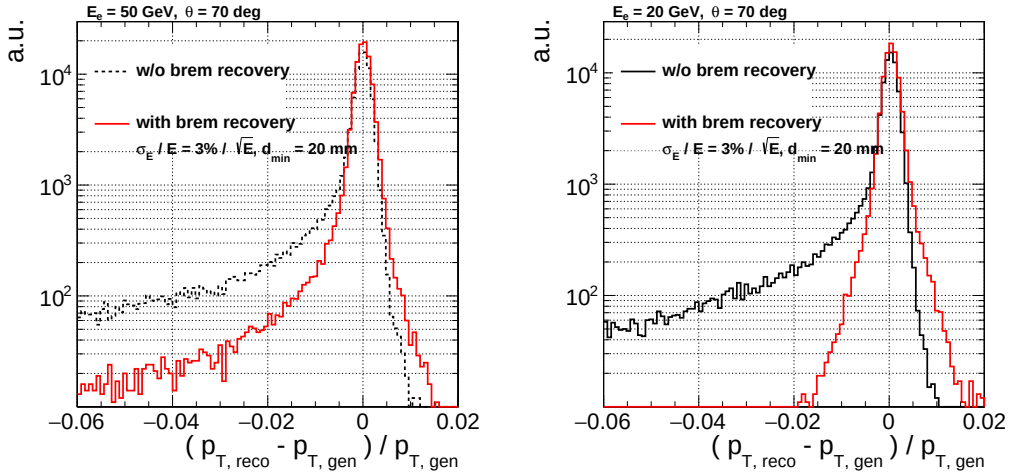

Fig. 8 Left: Relative momentum resolution for (left) 50 GeV and (right) 20 GeV electrons emitted at $\theta = 70°$, without (dashed histogram) and with (full histogram) bremsstrahlung recovery. The recovery procedure assumes a calorimeter resolution of $3\%/\sqrt{E}$, a minimal $R\phi$ distance of 20 mm, and an energy threshold of 10 MeV.

Crystal calorimeters offer the possibility to reach an exquisite energy resolution, with a Moliere radius $R_M \sim 2$ cm, a transverse granularity of 1×1 cm^2 or better, and some possibilities for longitudinal segmentation. The separation of close-by electromagnetic showers that state-of-the-art reconstruction algorithms can offer, depending on the granularity, will have to be investigated in full simulation studies. Indications, from tracker measurements, that an electron is likely to have radiated a photon [4], will be used by the reconstruction algorithm and the separation power will be larger than what a stand-alone calorimeter shower reconstruction would achieve. While waiting for the outcome of these studies, a value of 25 mm for the d_{min} parameter is assumed to be a good guess for a crystal calorimeter. This choice leads to an effective energy resolution for electrons that is about $20 - 25\%$ worse than the momentum resolution of muons.

From the right panel of Fig. 7, one sees that the d_{min} parameter is not limiting the performance of the bremsstrahlung recovery for 20 GeV electrons at $\theta = 70°$. One could go up to 60 mm without degrading the performance, thanks to the large bending of the electrons, and such a large value of d_{min} should be well within the reach of the calorimeters that are considered for FCC-ee. On the other hand, an efficient bremsstrahlung recovery for higher energy electrons, for example for 50 GeV central electrons, requires the parameter d_{min} to be smaller than about 25 mm. It should be noted that, would the magnetic field be increased from 2 T to 3 T, which may be possible at $\sqrt{s} = 240$ GeV, the separation between electrons and the radiated photons would increase by 50%: the "threshold" at ~ 30 mm seen in the left panel

[4] For example, while the GSF tracking may not provide a good resolution for the pre-brem electron, it can be good enough to show, from a comparison of the track momentum at the ECAL entrance and at the interation point, that a bremsstrahlung emission has likely occurred.

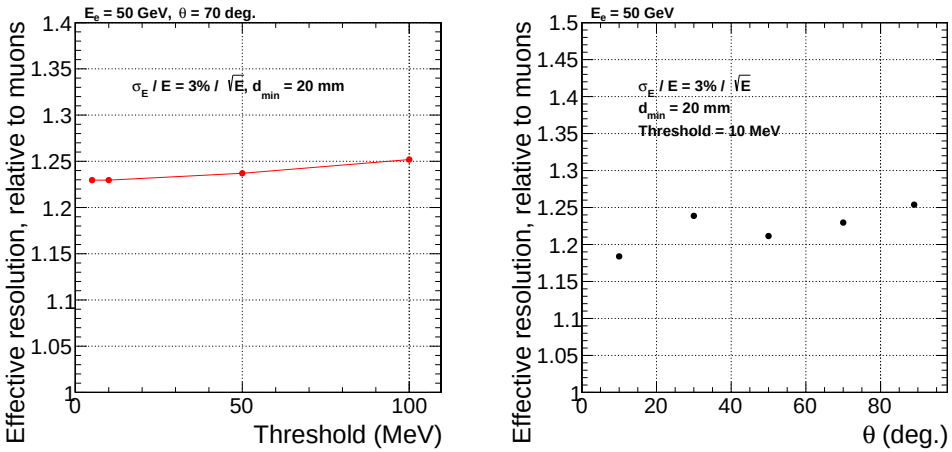

Fig. 9 Left: Effective resolution of electrons relative to the muon momentum resolution, obtained with bremsstrahlung recovery, as a function of the energy threshold below which the photons are not reconstructed, for electrons of 50 GeV emitted at $\theta = 70°$. Right: Angular dependence of the relative effective momentum resolution of electrons of $E_e = 50$ GeV, for a threshold of 10 MeV. In both cases, the recovery procedure assumes a calorimeter resolution of $3\%/\sqrt{E}$ and a minimal $R\phi$ distance of 20 mm.

of Fig. 7 would be "pushed" to $\sim$ 45 mm, such that the recovery for electrons from $Z(ee)H$ events would be much easier.

It should be reminded that, in the studies presented here, the last barrel layer of silicon is at a radius of 5.8 cm. In the IDEA detector, a "silicon wrapper" is present between the drift chamber and the ECAL. It will be a source of bremsstrahlung emissions which will not be recovered, but that is not an issue since, if an electron only radiates a photon in the wrapper, the tracker would measure the pre-brem electron momentum. More importantly, the IDEA barrel vertex detector consists of an inner and an outer part, the latter consisting of two layers of silicon at radii of 13 and 31 cm [10]. Bremsstrahlung emissions in the outermost layer would lead to photons that hit the ECAL at only $\sim$ 20 mm from the electron impact point, for 50 GeV central electrons bending in a 2 T field, as can be seen from the lower row of plots in Fig. 6. That may be too small for the reconstruction algorithm to properly resolve the photon shower. On the other hand, for such cases, the pre-brem track would be measured with a larger lever-arm, such that the GSF tracking may rescue the resolution for electrons emitting a photon in this outermost silicon layer.

5 Summary

For the DELPHES IDEA detector simulations made for the mid-term review studies, it has been assumed that, with a recovery of bremstrahlung photons, the effective resolution of electrons would be 25% worse than the muon resolution. While detailed full simulations are needed to ascertain this assumption, the studies detailed in this note

indicate that this target is not unrealistic. Consequently, in DELPHES, the momentum resolution of electron tracks is rescaled by a flat factor of 1.25, with respect to what is determined for muons of the same momentum and angle. In addition, DELPHES runs a simple "particle-flow" reconstruction step, whereby the measurement of the electron track momentum is combined with the measurement of the energy that the (post-brem) electron deposits in the ECAL. This combination improves further the electron resolution. The expected resolution at $\theta = 90°$ for electrons reconstructed with the bremsstrahlung recovery procedure is shown in Fig.10 (orange curve) and, by construction, is 25 % worse than standalone muons (blue curve). The resolution combining brem recovery and standalone ECAL reconstruction (green) is shown in dashed red [5]. The ECAL measurement of the electron track improves substantially the resolution for large momenta $p > 40$ GeV.

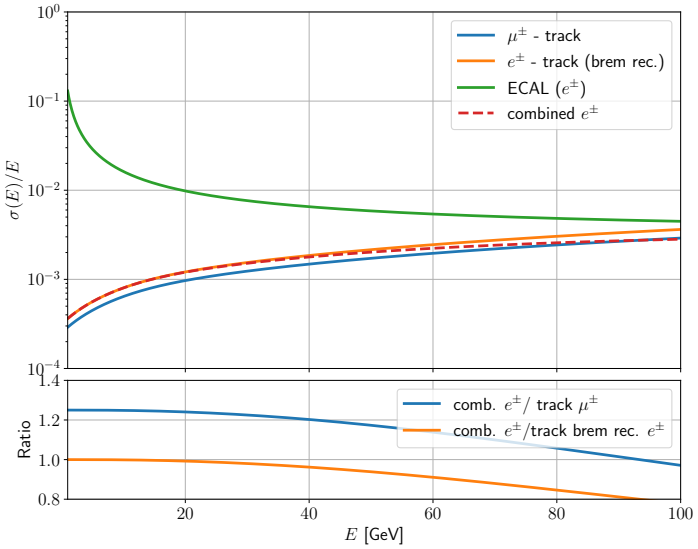

Fig. 10 Comparison of the expected resolution for muon tracks, electron tracks with the bremsstrahlung recovery procedure described in this note, standalone ECAL electron reconstruction, and the resolution obtained by combining the calorimeter standalone and the bremsstrahlung recovery.

Acknowledgements

This work has been partly supported by the Future Circular Collider Innovation Study (FCCIS) project, that has received funding from the European Union's Horizon 2020 research and innovation programme under grant No 951754.

[5] The standalone ECAL reconstruction assumes all the electron energy is deposited in the calorimeter, which is an approximation and does not account for the energy that is lost by bremsstrahlung.

References

[1] F. Bedeschi, L. Gouskos, M. Selvaggi, Jet flavour tagging for future colliders with fast simulation. Eur. Phys. J. C **82**(7), 646 (2022). https://doi.org/10.1140/epjc/s10052-022-10609-1. arXiv:2202.03285 [hep-ex]

[2] N. Bacchetta, et al., CLD – A Detector Concept for the FCC-ee (2019). arXiv:1911.12230 [physics.ins-det]

[3] J. Eysermans, A. Li, G. Bernardi. Higgs boson mass and model-independent ZH cross-section at FCC-ee in the di-electron and di-muon final states (2023). Preprint at https:xxx

[4] M. Dam. LFV processes involving tau leptons: FCC-ee perspectives (talk) (2020). https://indico.fnal.gov/event/44457/contributions/191705/attachments/131845/161604/Snowmass-clfv-200723.pdf

[5] R. Fruhwirth, Track fitting with non-Gaussian noise. Comput. Phys. Commun. **100**, 1–16 (1997). https://doi.org/10.1016/S0010-4655(96)00155-5

[6] R. Fruehwirth, S. Fruehwirth-Schnatter, On the treatment of energy loss in track fitting. Comput. Phys. Commun. **110**, 80–86 (1998). https://doi.org/10.1016/S0010-4655(97)00157-4

[7] W. Adam, R. Frühwirth, A. Strandlie, T. Todorov, Reconstruction of electrons with the gaussian-sum filter in the CMS tracker at the LHC. Journal of Physics G: Nuclear and Particle Physics **31**(9), N9–N20 (2005). https://doi.org/10.1088/0954-3899/31/9/n01. URL https://doi.org/10.1088%2F0954-3899%2F31%2F9%2Fn01

[8] M.T. Lucchini, W. Chung, S.C. Eno, Y. Lai, L. Lucchini, M.T. Nguyen, C.G. Tully, New perspectives on segmented crystal calorimeters for future colliders. JINST **15**(11), P11005 (2020). https://doi.org/10.1088/1748-0221/15/11/P11005. arXiv:2008.00338 [physics.ins-det]

[9] Separation of two overlapped electromagnetic or electromagnetic-hadronic showers in calice (2017). https://twiki.cern.ch/twiki/pub/CALICE/CaliceAnalysisNotes/CAN-057.pdf

[10] F. Palla. Talk presented at the London FCC week (2023). https://indico.cern.ch/event/1202105/contributions/5385347/attachments/2660171/4608255/FCC%20week%202023%20London.pdf